Nuclear Engineering and Design 239 (2009) 395–407

Contents lists available at ScienceDirect

Nuclear Engineering and Design

journal homepage: www.elsevier.com/locate/nucengdes

An innovative research reactor design

Federico E. Teruel[a,b,*], Rizwan-uddin[a]

[a] Department of Nuclear, Plasma and Radiological Engineering, University of Illinois at Urbana-Champaign, Urbana, IL 61801, USA
[b] Centro Atómico Bariloche, CNEA, Bariloche 8400, Rio Negro, Argentina

ARTICLE INFO

Article history:
Received 23 July 2008
Received in revised form 14 October 2008
Accepted 31 October 2008

ABSTRACT

A new and innovative core design for a research reactor is presented. It is shown that while using the standard, low enriched uranium as fuel, the maximum thermal flux per MW of power for the core design suggested and analyzed here is greater than those found in existing state of the art facilities without detrimentally affecting the other design specs. A design optimization is also carried out to achieve the following characteristics of a pool type research reactor of 10 MW power: high thermal neutron fluxes; sufficient space to locate facilities in the reflector; and an acceptable life cycle. In addition, the design is limited to standard fuel material of low enriched uranium. More specifically, the goal is to maximize the maximum thermal flux to power ratio in a moderate power reactor design maintaining, or even enhancing, other design aspects that are desired in a modern state of the art multi-purpose facility. The multi-purpose reactor design should allow most of the applications generally carried out in existing multi-purpose research reactors. Starting from the design of the German research reactor, FRM-II, which delivers high thermal neutron fluxes, an azimuthally asymmetric cylindrical core design with an inner and outer reflector, is developed. More specifically, one half of the annular core ($0 < \theta < \pi$) is thicker than the other half. Two variations of the design are analyzed using MCNP, ORIGEN2 and MONTEBURNS codes. Both lead to a high thermal flux zone, a moderate thermal flux zone, and a low thermal flux zone in the outer reflector. Moreover, it is shown that the inner reflector is suitable for fast flux irradiation positions. The first design leads to a life cycle of 41 days and high, moderate and low (non-perturbed) thermal neutron fluxes of 4.2×10^{14} n cm^{-2} s^{-1}, 3.0×10^{14} n cm^{-2} s^{-1}, and 2.0×10^{14} n cm^{-2} s^{-1}, respectively. Heat deposition in the cladding, coolant and fuel material is also calculated to determine coolant flow rate, coolant outlet temperature and maximum fuel temperature under steady-state operating conditions. Finally, a more compact version of the asymmetric core is developed where a maximum (non-perturbed) thermal flux of 5.0×10^{14} n cm^{-2} s^{-1} is achieved. The core life of this more compact version is estimated to be about 23 days.

1. Introduction

Neutrons are used for research and in many industrial and medical applications. Sources capable of producing high neutron fluxes with desired spectrum are needed to perform material research, radiography and cancer therapy among other important uses. Research reactors (RRs) are one possible source of neutrons. The flux and spectrum of neutrons and availability of irradiation facilities determine the types of applications and, therefore, usefulness of a reactor. New RRs continue to be developed. Restriction on level of enrichment in these reactors has led to some constraints on their designs. However, with improved simulation and design tools, it is now possible to explore design features that would have been difficult to analyze with an earlier generation of design tools, and thus it is becoming possible to mitigate at least some of the restrictions posed by fuel enrichment levels by more thoroughly exploring the design parameter space than was possible earlier. The goal of this study was to design a new RR possibly incorporating design features that have not been included in earlier designs. Work presented here is built upon preliminary studies reported in (Teruel and Rizwan-uddin, 2005) and (Teruel and Rizwan-uddin, 2006). Desirable operational and geometric features in a modern RR are discussed first.

Maximum neutron flux is an important parameter for modern RRs. High neutrons flux levels allow the successful operation of devices such as cold neutron sources, but greatly increase the complexity of the reactor and the magnitude of the project. Table 1 shows maximum thermal neutron fluxes found in the reflector (MTF in units of n cm^{-2} s^{-1}) and some other characteristics of some

* Corresponding author at: Centro Atómico Bariloche, CNEA, Bariloche 8400, Rio Negro, Argentina. Tel.: +54 2944 445166.
E-mail address: teruel@cab.cnea.gov.ar (F.E. Teruel).

0029-5493/$ – see front matter © 2008 Elsevier B.V. All rights reserved.
doi:10.1016/j.nucengdes.2008.10.025

Table 1
Characteristics of some of the multi-purpose RRs.

RR (location)	MTF $\times 10^{14}$ (n cm^{-2} s^{-1})	MFF $\times 10^{14}$ (n cm^{-2} s^{-1})	Enrichment	Core life (days)	Power (MW)	MTF MW^{-1} $\times 10^{13}$
HFIR (USA)	25.5	10.0	HEU	23	85	3.0
FRM-II (Germany)	8.0	5.0	HEU	52	20	4.0
HANARO (Korea)	4.5	3.0	LEU	28	30	1.7
JRR-3M (Japan)	2.0	1.4	LEU	26	20	1.0
OPAL[a] (Australia)	3.0[b]	2.1	LEU	≈30	20	1.5

MTF and MFF indicate maximum thermal flux and maximum fast flux, respectively.
[a] Recently completed.
[b] Perturbed.

of the larger size multi-purpose pool type RRs that are currently operating or under construction (IAEA, 1999). Since the MTF is proportional to the power of the reactor, the MTF normalized with power (MTF per Megawatt, MTF MW^{-1}, column 7) is a parameter that allows comparison of maximum fluxes for reactors with different power levels. As can be seen from Table 1, the German FRM-II reactor (FRM-II, 2008) has the highest MTF MW^{-1} in this group of reactors. This RR has been designed to optimize beam applications. Despite the fact that it was designed to operate with 93% enrichment, the compact construction of its fuel element is an attractive feature. This core produces a maximum thermal neutron flux of 8×10^{14} n cm^{-2} s^{-1} or 4×10^{13} n cm^{-2} s^{-1} MW^{-1} (undisturbed) at a distance of 12 cm from the surface of the fuel element. Another reactor, OPAL (2008), is a state of the art multi-purpose RR facility that allows cold/thermal/hot beams research, radioisotopes production, silicon doping, etc. These capabilities are achieved with a MTF of about 3.0×10^{14} n cm^{-2} s^{-1} (perturbed) (IAEA, 1999). Suggested by the MTF and the capabilities found in the OPAL reactor, together with the maximum thermal flux per unit power achieved by the FRM-II reactor, a power level of 10 MW with a desirable MTF of 4×10^{14} n cm^{-2} s^{-1} is selected as design specification. This power level is such that the reactor can be easily placed in a national laboratory, university or even in a commercial environment.

Economic constraints have pushed new reactors to be multi-purpose. Any future research reactor is much more likely to be a multi-purpose reactor with educational, research and industrial applications jointly providing the operational cost. Hence, the design is expected to have irradiation facilities for thermal as well as fast end of the neutron energy spectrum. Efficient use of all neutrons produced has led to the use of heavy water tanks (Ryskamp et al., 1991). These experiences have contributed to the choices made in this study.

Modern multi-purpose RRs are characterized by small and compact cores designed to facilitate the leakage of neutrons to the reflector, where they can be used for different purposes. For example, 70% of neutrons produced in the FRM-II design escape to the reflector (FRM-II, 2008). Competing demands for high neutron flux and long core life have led several RR designs to rely on HEU as fuel. However, future RR designs are likely to be restricted to a maximum enrichment of 20% (see the Reduce Enrichment for Research and Test Reactors program, RERTR, 2008). Hence, the fuel for the designs considered here is restricted to maximum enrichment of 20%, and a 30–40-day operation-cycle is considered sufficient for most applications (see Table 1).

Another desirable feature of a RR core design is the ability to have access to neutrons with soft as well as with harder spectrum. This capability enhances the versatility of the design and provides spectrum for a more diverse use of the facility. While soft spectrum neutrons may be needed for certain experiments, fuel material testing for example, may require access to harder neutron spectrum. In general, low energy neutrons are easily accessible. Providing access to fast neutrons is on the other hand often requires optimization between accessibility to fast neutrons and loss in highest accessible flux. Locations close to the boundary between the core and the reflector outside the core may be tapped to have access to fast flux, but perturb the thermal neutron flux in other parts of the reflector. An annular cylindrical core—with access to fast neutrons in the inner region and thermal neutrons in the outer reflector—is often found to be the ideal compromise. The inner region of this annular cylindrical core close to the inner face of the fuel element (FE) may be used for irradiation positions for neutrons with relatively harder spectrum. These inner irradiation positions are expected to only slightly affect the neutron fluxes in the outer reflector. The inner region may, in addition to irradiation positions (IP), contain structural material, an inner reflector, control mechanisms and coolant channels. Positioning these in the inner cavity minimizes the effect on the level of thermal flux in the outer reflector.

The objective of this work is to analyze and optimize different core configurations for a multi-purpose, pool type RR to maximize neutron fluxes delivered to the reflector. Based on the observations stated in the previous paragraphs, the desirable general features and some specific design specs of the RR are:

- Pool type reactor with a central core and heavy water as reflector (with reasonable amount of free space available in the reflector to position facilities/devices),
- Annular core allowing irradiation positions in the inner region with spectrum that is harder than that in the outer reflector.
- An inner region no smaller that 314 cm^2 (equivalent to a cylinder of 10 cm of radius).
- Thermal power of 10 MW with a MTF greater than 4×10^{14} n cm^{-2} s^{-1}.
- Standard fuel material with enrichment no higher than 20%.
- Core life longer than 40 days.

Remainder of this paper describes the steps toward the realization of this design goal. Preliminary calculations for the core shape and dimensions that satisfy the stated goals are carried out in Section 3 of the paper using a homogeneous representation for the core. This greatly simplifies the problem and since the MTF occurs in the reflector and is therefore expected to be only slightly affected by the exact modeling of the core, even a homogeneous representation of the core is expected to lead to representative results for the MTF. [This claim is first supported by a qualitative comparison between fluxes calculated with a homogeneous representation of the FRM-II core and those reported in literature for a heterogeneous core (Section 2).] Further on, a parametric study with elementary variations of the FRM-II core geometry is carried out. The conclusion drawn from this study is that the required specs of the proposed design cannot be achieved with this geometry under the assumed constraints. However, based on the results of these studies, numerical experiments are then performed with asymmetric annular cores in Section 4. The asymmetry in the vertical core is in the azimuthal direction due to different outer radii of the two segments of the annular cylinder. A design that satisfies the stated goals is obtained with the asymmetric annular geometry in the expanded design

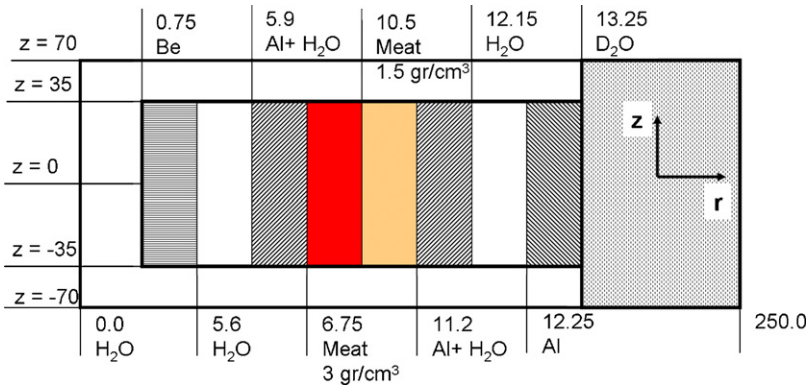

Fig. 1. Schematic diagram of the simplified model of the FRM-II (not to scale) in the r–z plane. All numbers are dimensions in cm.

space. The design is naturally characterized by an asymmetric neutron flux distribution in the reflector. This is an unexpected positive feature in a multi-purpose RR because though many applications require high neutron fluxes others need moderate or low neutron fluxes, and therefore, different parts of the reflector may be used for different applications according to their neutron/gamma flux level requirements. As a result of the study presented in Section 4, a standard asymmetric design is selected as a prototype for further study.

Core life and reactivity variations of the prototype are studied in Section 5 under different core configurations. The homogeneous representation of the core is next replaced by a more accurate heterogeneous model of the fuel elements. Neutron fluxes are recalculated for this detailed core, and steady-state thermo hydraulic analysis is carried out to evaluate parameters for safe operation of the standard design (Sections 6, 7 and 8). The analysis of the heterogeneous prototype shows that this new core design achieves the design goals, delivering maximum thermal fluxes per unit power that is greater than those found in existing state of the art facilities. Finally, the asymmetric model is further modified in Section 9 to explore the drop in core life with further increase in maximum neutron flux. By relaxing the requirement of an inner irradiation area, a more compact asymmetric core is modeled. Maximum thermal flux as well as core life is calculated, showing that for a 10 MW power reactor a MTF of 5.0×10^{14} n cm^{-2} s^{-1} can be achieved if a core life of about 23 days is acceptable.

2. Verification by modeling the FRM-II

MCNP version 5 (MCNP5, 2003) is used for all criticality calculations in this study. All MCNP calculations reported in this paper are *KCODE-type* calculations. The goal of this part of the study is two fold: to demonstrate that MCNP simulations yield results that are in agreement with earlier reported results; and to demonstrate that a homogeneous core model is sufficient to capture the primary characteristics of the design. Since data are available for the FRM-II reactor, it has been chosen as the test model.

The core of the FRM-II is a cylindrical fuel element that consists of 113 involute and curved fuel plates (Hanan et al., 1996; Bonning et al., 2004; FRM-II, 2008). The meat is made of U_3Si_2 in aluminum dispersion with two graded uranium densities (1.5 and 3.0 g cm^{-3}). For preliminary design optimization studies, the geometric details of the core are considered to be not essential and a homogeneous core model is deemed sufficient. This model is an annular cylindrical core (homogeneous mixture 17 vol.% fresh meat, 21 vol.% cladding and 62 vol.% coolant) with heavy water as external reflector and beryllium as internal one. The height of the active core region is 70 cm and a layer of 35 cm of light water was modeled above and below the core. The core is symmetric with respect to the mid plane ($z = 0$; where z is the axial direction) and in the azimuthal direction. Fig. 1 (not to scale) shows different material regions in the core and reflectors as well as their dimensions in centimeters (Hanan et al., 1996; Bonning et al., 2004). Note that two different uranium densities are modeled in the core: 3.0 g cm^{-3} from 6.75 to 10.5 cm and 1.5 g cm^{-3} from 10.5 to 11.2 cm in the radial direction. The outer radius of the core is 250 cm, and vacuum-boundary conditions are imposed over all external surfaces. No facilities are modeled in the reflector. For the simple FRM-II model simulation, 500 cycles of 1000 particles per cycle were simulated (standard deviation in k_{eff} is less than 0.0015).

Two cases are considered. The first one is a non-critical configuration shown in Fig. 1. The second one corresponds to a critical configuration of the system shown in Fig. 1 at the BOC. Criticality is achieved by replacing the inner reflector (beryllium) by a control rod (CR) composed of aluminum (0.75–5.35 cm) and hafnium (5.35–5.6 cm). This second case is simulated to evaluate possible variations in the radial profile of the neutron flux when control rods are inserted to achieve criticality. Fast and thermal (<0.625 eV) neutron flux distributions are tallied.

Fig. 2 shows the radial profiles for fast and thermal fluxes calculated at the central horizontal plane of the reactor (between $z = \pm 1$ cm) and rings of $\Delta r = 1$ cm for both cases mentioned above. The multiplication factor for the non-critical case is $k_{\text{eff}} = 1.202$. Dots in Fig. 2 show reference values of (non-perturbed) thermal fluxes in the reflector of the FRM-II reactor as reported in Glaser (2002) (see also FRM-II, 2008). The purpose of this comparison is not to show quantitative agreement between reference fluxes reported and the simplified model. It is presented to justify that a model based on a homogeneous description of the core yields enough details and sufficient qualitative fidelity to permit parametric studies to maximize the thermal flux in the reflector for different "FRM-II core type" configurations.

The effects on the thermal peak or MTF of changes in core configurations to identify design features that satisfy the stated goals of this program are investigated next.

3. Elementary variations of the FRM-II

Two major changes introduced in the core design of the FRM-II are: an inner region that is at least 314 cm^2; and meat material with enrichment lower than 20%. This implies that the new model should have a central zone for irradiation purposes of at least 10 cm of radius. Additionally, the fuel material is chosen to be U_3Si_2–Al of 4.8 gU/cm^3 with an enrichment of 20%. Note that this gives a U5 density of 0.95 g/cm^3 while the U5 density in the FRM-II RR

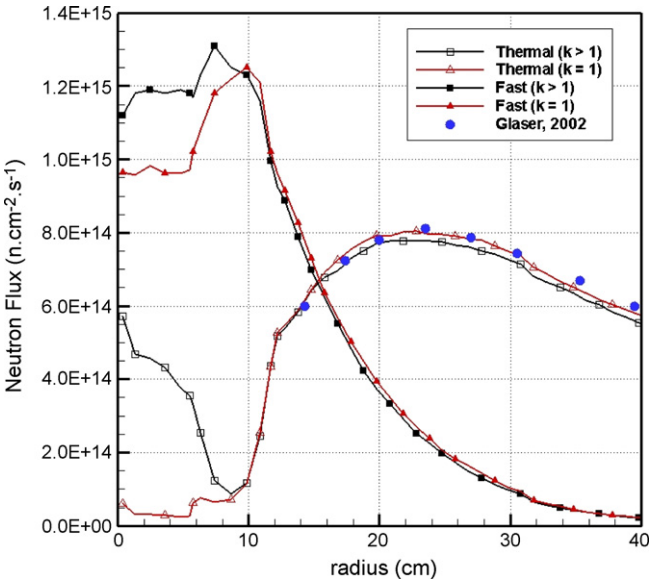

Fig. 2. Radial profile of thermal and fast neutron fluxes in the simplified model of the FRM-II. Case 1: BOC, $k > 1$; Case 2: BOC, $k = 1$ (by replacing Be reflector by a CR). Reference flux values for heterogeneous core simulation (Glaser, 2002).

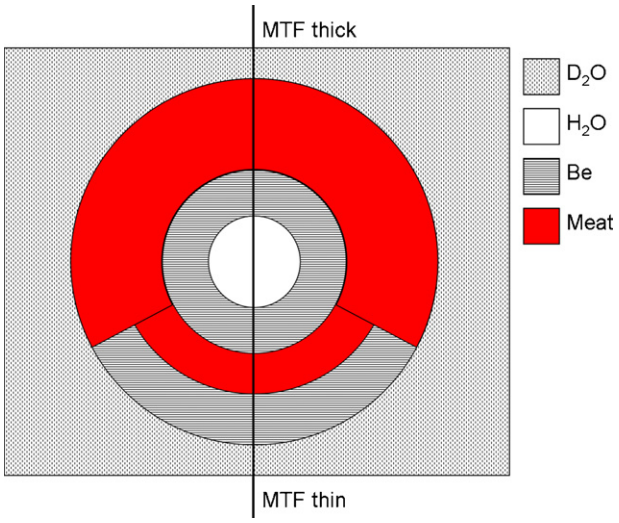

Fig. 3. Schematic diagram of the asymmetric cylindrical core.

is approximately equal to 2.5 g/cm^3. The modified model has the following features:

- Core: homogeneous, 17% volume meat (U_3Si_2–Al, 20% U5[1]), 21% cladding (Al-6061[1]) and 62% light water. 70 cm height.
- Inner region: beryllium (from 5 cm to inner core radius) and light water (from 0 to 5 cm of radius). 70 cm height.

The inner zone in this preliminary design is modeled as an inner reflector (Be), which increases excess reactivity at BOC, and acts as a channel of light water to allow the positioning of irradiation stations. All other dimensions are the same as those used in the basic FRM-II model (shown in Fig. 1). However, no gaps of water and/or structural material are modeled in this parametric study.

The first set of simulations was carried out to study the effect of the thickness and the inner radius of the cylindrical fuel element on the thermal neutron flux peak in the outer reflector. Multiplication factor and MTF are reported for 14 cases in Table 2. Meat thickness is varied between 2 and 7 cm, while the inner radius of the fuel element is varied between 10 and 16 cm. Recall that the goal is to achieve a MTF of 4×10^{14} n cm^{-2} s^{-1} in the heavy water reflector (or equivalently 4×10^{13} n cm^{-2} s^{-1} MW^{-1}). Fluxes are tallied in cylindrical rings with $\Delta r = 3$ cm in a slice about the central plane between $z = \pm 1.5$ cm. The amount of U5 contained in the entire core is also shown for comparison purposes. Note that the FRM-II core has approximately 0.375 kgU5/MW and a life cycle of about 52 days. Thermal neutron fluxes higher than 4×10^{14} n cm^{-2} s^{-1} are found with thinner fuel elements which, for a fixed power level, must operate at higher power density and also allow greater neutron leakage to the reflector. However, the excess reactivity of these assemblies is not enough to sustain a critical core for an acceptable period of time or, in some cases, even to produce it. All cases presented in Table 2 with MTF higher than the target value show excess reactivity at the BOC to be below 6% (Δk) (Cases I, II and VI). Considering that a Δk of at least 5% is needed to account for the negative reactivity introduced by facilities and devices located in the heavy water reflector, these assemblies cannot be expected to achieve the desired core life. In addition, irrespective of the size of the inner core radius, increasing the thickness of the core to increase life span reduces the MTF to below target. Note that FRM-II core is relatively small leading to a high power density. Moreover, more than 70% of the neutrons produced in the core are leaked out. The amount of U5 necessary to sustain a critical reaction for the core life is assured by a high enrichment.

Clearly, this core geometry under the enrichment constraints is incapable of simultaneously delivering the target MTF and core life. In addition, the parametric study reported in Table 2, as expected, shows that thick cores may have an acceptable core life, and thin ones produce the expected thermal neutron flux peak. Consequently, the geometry is varied and numerical experiments are carried out with asymmetric cores, seeking a core that may produce the target MTF only in a specific region in the reflector. Moderate thermal neutron fluxes suitable for applications such as industrial processing would be acceptable in the remainder of the reflector. The core must also have an inner irradiation zone and an acceptable core life as stated in the design goals.

4. Novel asymmetric core model

The asymmetric core shown in Fig. 3 consists of two segments: a thinner part of angle θ, and a thicker part of angle $(2\pi - \theta)$. There is beryllium and light water in the center as in the symmetric model. Thinner meat section is padded with beryllium to make its outer radius equal to that of the thicker meat section. Inner radius is kept the same in both segments to make the neutron spectrum harder in the inner region. The neutron flux in this case is not expected to be symmetric. Due to asymmetry, instead of an evenly (in azimuthal direction) distributed thermal flux in the reflector, this core is expected to lead to thermal fluxes that vary with θ for fixed r and z. For the central plane ($z = 0$) and for a fixed angle θ (i.e. a radial line in the central horizontal plane), a maximum of the thermal flux is obtained in the reflector. The maximum (MTF) and minimum of these maximum thermal fluxes are on a line passing through the center of the thick and thin core segments (vertical line in Fig. 3).

A set of simulations were carried out to parametrically study the thermal neutron flux peak as a function of the outer radii of both core sections and the aperture angle of the thinner segment. First,

[1] Equivalent impurities are accounted considering 8.5 ppm and 17 ppm of atoms of B_{10} for the fuel and cladding, respectively.

Table 2
MTF as a function of thickness and inner radius of the (azimuthally symmetric) cylindrical fuel element.

Case	I	II	III	IV	V	VI	VII
Inner core radius (cm)	10	10	10	10	10	12	12
Thickness (cm)	2	3	4	6	7	2	3
Multiplication factor	0.982	1.059	1.119	1.207	1.238	1.010	1.100
MTF ($\times 10^{14}$)	4.98	4.07	3.60	2.81	2.42	4.45	3.72
U5 ratio to FRM-II (kg/kg)[a]	0.48	0.75	1.04	1.70	2.06	0.57	0.88
Case	VIII	IX	X	XI	XII	XIII	XIV
Inner core radius (cm)	12	12	14	14	14	16	16
Thickness (cm)	4	6	2	3	4	2	3
Multiplication factor	1.151	1.234	1.052	1.124	1.183	1.147	1.076
MTF ($\times 10^{14}$)	3.15	2.38	3.97	3.25	2.89	2.99	3.71
U5 ratio to FRM-II (kg/kg)[a]	1.22	1.96	0.65	1.01	1.39	0.74	1.14

[a] Normalized with power.

Table 3
Parametric study for the asymmetric cylindrical core (fixed core inner radius of 10 cm).

Case	I	II	III	IV	V	VI
Thickness, thin segment (cm)	6	4	2	0	6	4
Aperture angle, thin section (°)	60	60	60	60	120	120
Multiplication factor	1.233	1.232	1.216	1.201	1.231	1.205
MTF thick ($\times 10^{14}$)	2.53	2.77	2.77	2.81	2.48	2.93
MTF thin ($\times 10^{14}$)	2.60	2.56	2.74	2.76	2.77	2.88
MTF thick/MTF thin ratio	0.97	1.08	1.01	1.02	0.89	1.02
U5 ratio to FRM-II (kg/kg)[a]	1.73	1.64	1.55	1.49	1.68	1.49
Case	VII	VIII	IX	X	XI	XII
Thickness, thin segment (cm)	2	0	6	4	2	0
Aperture angle, thin section (°)	120	120	180	180	180	180
Multiplication factor	1.192	1.157	1.224	1.195	1.162	1.107
MTF thick ($\times 10^{14}$)	3.35	3.65	2.81	3.28	3.75	4.45
MTF thin ($\times 10^{14}$)	2.78	2.84	2.63	2.74	2.76	2.61
MTF thick/MTF thin ratio	1.20	1.28	1.07	1.20	1.36	1.71
U5 ratio to FRM-II (kg/kg)[a]	1.33	1.19	1.63	1.34	1.10	0.89

[a] Normalized with power.

to assess the quantitative impact of the asymmetry on the maximum thermal flux, the thickness of the thicker section is kept fixed at 7 cm (inner and outer radii equal to 10 and 17 cm, respectively), and the results are tabulated in Table 3 for three different aperture angles (60°, 120° and 180°) and for four different thickness of the thin segment (6, 4, 2 and 0 cm). Table 3 shows in addition to the multiplication factor at BOC, the amount of U5, and the maximum thermal flux obtained along a radial line passing through the center of the thicker and thinner core sections in the $z = 0$ plane (fluxes calculated in cylindrical cells, $\Delta r = 3$ cm, $\Delta\theta = 10°$, $z = \pm 1.5$ cm). Results show that by increasing the asymmetry of the core (i.e. increasing the aperture angle and/or reducing the thickness of the thin section) the difference between the MTF calculated outside the thinner and thicker segments of the core increases (see the MTF thick/MTF thin ratio in Table 3). Note that because neutron fluxes are calculated every 3 cm, maximums fluxes are calculated approximately, and for this reason, there is some noise in the results shown for this ratio. While for symmetric cases presented in Table 2, MTF greater than 4.0×10^{14} cm^{-2} s^{-1} are achieved only with reactivity excess less than 6% (Δk), one of the asymmetric model achieves this MTF with reactivity excess greater than 10% (Δk, Case XII in Table 3). Thus, the asymmetric core is able to deliver the desired MTF with a reactivity excess that may be sufficient to satisfy the design requirement for core life. Cores with half-thick and half-thin segments (180° aperture) yield the highest MTF. Moreover, the MTF increases as the thin segment becomes thinner. [Note that the MTF occurs on the thick side of the core. The increase in the MTF when the thin side is made even thinner is due to increased power density in the thicker section necessitated by the fixed total power level.] Based on these observations further parametric studies are carried out for asymmetric cores that are half thick and half thin. The thickness of the thin segment of the core is kept at 1 cm to

Table 4
Parametric study for the asymmetric cylindrical core (half-thick and half thin core with thickness of the thin segment fixed at 1 cm).

Case	I	II	III	IV	V	VI
Inner radius (cm)	10	10	12	12	14	14
Thickness, thick segment (cm)	7	8	6	7	5	7
Multiplication factor	1.145	1.176	1.143	1.173	1.134	1.172
MTF thick ($\times 10^{14}$)	4.04	3.69	3.90	3.75	4.25	3.59
MTF thin ($\times 10^{14}$)	2.79	2.57	2.62	2.24	2.52	2.15
MTF thick/MTF thin ratio	1.45	1.44	1.49	1.67	1.69	1.67
U5 ratio to FRM-II (kg/kg)[a]	0.99	1.16	0.97	1.14	0.91	1.29

[a] Normalized with power.

Table 5
Reactivity effects due to changes in the configuration of the inner-irradiation zone (changes involve entire active core height of 70 cm).

Case	k_{eff} at BOC (±0.004)
I – Base case (Case I, Table 4)	1.145
II – Critical base case with hafnium control rod (6.5–6.8 cm of radius)	1.003
III – Inner region filled with Be (r < 10 cm)	1.203
IV – 16 fast IPs plus 4 thermal IPs (filled with light water, Ø = 1.3 cm and Ø = 3.0 cm, respectively, Fig. 4)	1.183
V – Same as Case IV but IPs filled with heavy water	1.205
VI – Black absorber in all 16 fast IPs (z = ±5 cm)	1.070
VII – Case IV with Zry-4 ring (8 < r < 10 cm)	1.151

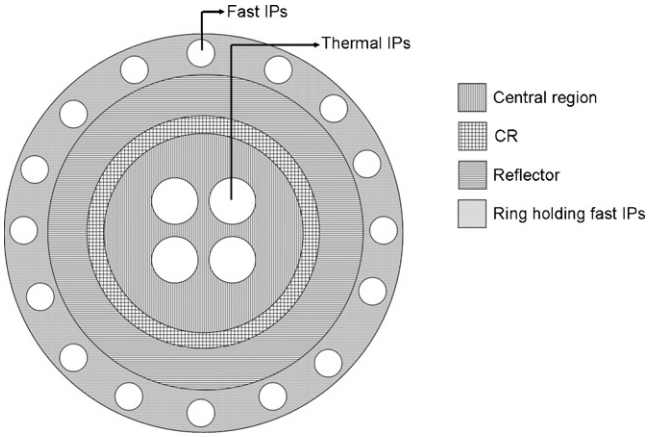

Fig. 4. Schematic diagram of the inner region for cases identified in Table 5.

improve reactivity excess and to increase fast neutron population in the inner region.

Table 4 shows the results of the final parametric study of the asymmetric model. Inner radius of the core and the thickness of the thick segment are varied. In all six cases shown in Table 4, MTF greater than or close to the target value are achieved together with reactivity excess that may be sufficient for the desired core life. Case I in Table 4 shows a MTF above the target value and also a high value of the MTF outside the thin segment. Additionally, reactivity excess value is higher than that calculated for the other case that achieves the target MTF (Case V). Therefore, Case I in Table 4 is selected as a preliminary conceptual design of the core. This model is analyzed in more detail in the following sections for core life and to assess the effects on reactivity of different configurations of the inner region.

5. Inner cavity, reactivity sensitivity and core life

The main purpose of the inner region is to equip the design with capability to irradiate materials with fast spectrum and, as in the FRM-II case, to provide a fine mechanism to control the reactor during its life cycle (minimizing flux perturbations in the outer reflector). Naturally, the initial reactivity of the case selected as preliminary conceptual design is strongly dependant on the material and configuration chosen for this region. Excess reactivity at BOC is hence calculated for different configurations of the inner region to study its possible impact on the core life. Simulations were carried out using the MCNP code, with 250 active cycles of 1000 particles per cycle. In all cases, the standard deviation in k_{eff} is less than 0.0025. Table 5 shows the variation in the multiplication factor at BOC for different configurations of the inner-irradiation zone (all modifications cover the entire 70 cm axial span of the core). Case I in Table 5 shows the base case (Case I in Table 4). A control rod of sufficient thickness is introduced in Case II to compensate for the excess reactivity at BOC, leading to a k_{eff} of about one. Light water in the central cavity is replaced by beryllium in Case III, leading to additional excess reactivity at BOC. Case IV (Fig. 4, not to scale) is of particular interest because the inner region is modeled as a Be reflector with 20 holes to serve as irradiation positions (IPs); 16 IPs close to the inner face of the reactor (Ø = 1.3 cm) for fast flux and 4 IPs (Ø = 3.0 cm) for thermal neutrons. Some reactivity is also gained in this case because the total amount of light water in the model is less than that in the base case. Case V is similar to Case IV except that the IPs are filled with heavy water. Case VI is similar to Case IV but with a black absorber modeled in all 16 fast IPs between z = ±5 cm. Case VII is also similar to Case IV but with a ring of Zry-4 between the inner reflector and the core, where the fast IPs are located. This configuration may improve the fast/thermal flux ratio in the fast IPs. As expected, Cases III and V show the highest excess reactivity at BOC. k_{eff} at BOC for other cases quantify the impact of these design options.

Additional holes for irradiation positions or control devices may be located in the inner region or in the region filled with beryllium to make the outer radius of the thin core segment equal to that of the thick section. Hence, this configuration presents a large spectrum of possibilities to control the core and irradiate materials in the inner irradiation zone, simultaneously assuring an acceptable core life. Note that some IP locations can be removed to increase reactivity up to the upper limit corresponding to Case III (Table 5).

Core life is another parameter that has been chosen as a design constraint and acts as a limiter on the level of the MTF. Consequently, core life is calculated at this stage of the conceptual design process. Core life of Cases I and IV in Table 5 was estimated using MONTEBURNS 2.0 (Poston and Trellue, 1999). This computational tool links MCNP transport code and ORIGEN2 burnup code (Croff, 1980). The MCNP model was 1/4 of the real core and each MCNP run involved 350 active cycles of 1000 particles (standard deviation in k_{eff} was lower than 0.002 and tallies in core cells passed all statistical checks). MCNP calculations are performed at 45 °C and heavy and light water densities are evaluated at this temperature. As ORIGEN2 is a zero dimensional code, the 1/4 core MCNP model was divided into 36 different regions to account for the variation of the burnup with position. The thinner part of the core was divided into nine regions of equal volume (three angular and three axial intervals). The thick segment of the core was divided into 27 regions, as in the thinner case for θ and z, and additionally it was split also in three different radial zones (10–12.33, 12.33–14.66, 14.66–17 cm). Burnup calculations were carried out for 50 days and the neutron fluxes were actualized (MCNP calculation) every 2 days. Forty burnup steps are performed in ORIGEN2 every 2 days with 1 predictor step every 2 days. The PWRU library was used in ORIGEN2. Finally, the fractional importance in MONTEBURN 2.0 was chosen to be equal to 1.0E−5. Fig. 5 shows the variation of k_{eff} as a function of time for Cases I and IV in Table 5.

It is clear from Fig. 5 that reactivity variation with time is not strongly dependant on the configuration of the inner region. Therefore, core life for other configurations of the inner region may be estimated based on Fig. 5. Moreover, no devices/facilities have been modeled in the outer reflector and this is expected to have a slight influence on the reactivity change with burnup. However, the marginal reactivity necessary to account for these devices is clearly important in estimating the core life. Hanan et al. (1996) and Bonning et al. (2004) set the value of marginal reactivity due to temperature effects and facilities in the reflector equal to 6–9%

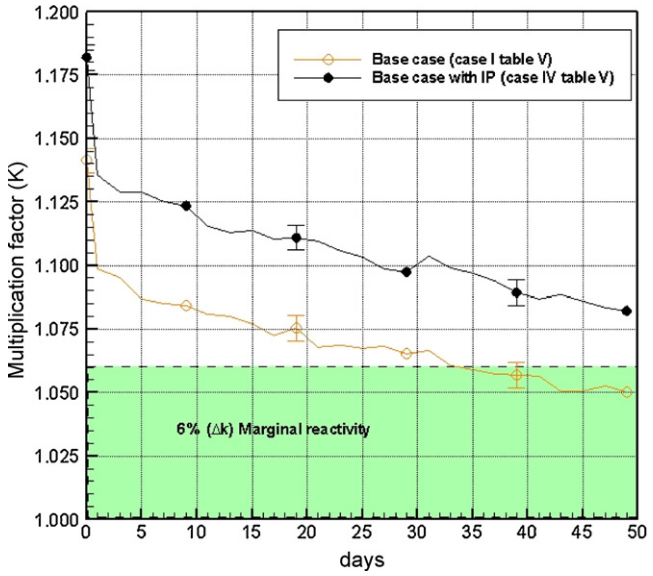

Fig. 5. Multiplication factor for the burnup of base case with and without IPs in the inner region.

(Δk) for the FRM-II reactor, while a value of 5% (Δk) is chosen for the advance neutron source design (Ryskamp et al., 1991). After 41 days, Cases I and IV, respectively show an available marginal reactivity of $\Delta k = 5.3 \pm 0.5\%$ and $\Delta k = 8.3 \pm 0.5\%$. Despite the fact that both cases achieve the desired core life of 40 days, an even longer cycle can easily be obtained by replacing some IPs by Be. It is important to mention that this marginal reactivity is strongly dependant on the number and orientation of beams located in the reflector since they displace large quantities of heavy water. A marginal reactivity of 6% (Δk) is shown in Fig. 5. An error in k_{eff} equal to two standard deviations is also shown in the calculated data (± 0.004).

6. Detailed core model – the standard design

The homogeneous core model resulted in a useful tool to develop a preliminary conceptual design capable of achieving the design goals. However, further analysis using a detailed heterogeneous model of the core is necessary to assure more quantitatively accurate results and to determine additional parameters such as those necessary for thermal hydraulic analysis. Case IV in Table 5 is selected for further analyses. This configuration will henceforth be referred to as the *standard design*. It is chosen for detailed analyses not only because it fulfills design specs but also because its inner cavity has a large number of IPs with different flux characteristics. The standard design is modeled as a group of 10 heterogeneous fuel elements (FEs), five for each azimuthal half of the core. Each FE of the thick segment of the core is made of 19 cylindrical fuel plates; the FE of the thinner segment consists of 3 fuel plates (Fig. 6). The inner region is modeled as in Case IV in Table 5, with 16 fast IPs and 4 thermal IPs. Table 6 shows dimensions and materials for the standard design and for the inner region (fuel plate dimensions are the same as those in the FRM-II reactor).

The addition of structural material in the standard design configuration, plus small changes in the percentage of light water, cladding and meat compared to the homogeneous case are expected to lead to reactivity changes. Therefore, the initial excess reactivity is recalculated for the heterogeneous core for different configurations of the inner region and for the base case (light water filling IPs). All calculations are carried out assuming an operating temperature of 65 °C for the meat and 45 °C for the rest of the reactor. Results are shown in Table 7. As expected, initial (BOC) reactivity of the heterogeneous core is found to be slightly lower than that calculated for the homogeneous one. As the excess reactivity of the base case is 16.8% (Δk), this core is expected to have a marginal reactivity of $\Delta k = 6.8 \pm 0.5\%$ after 41 days of operation (based on Fig. 5, case with IPs). Criticality is achieved in the heterogeneous model by positioning a cylindrical shell shaped hafnium CR with inner and outer radii of 6.1 and 6.7 cm, respectively. The shell-shaped control rod spans the entire height of the FE. Cases IV and V show the excess reactivity at BOC with air filling the IPs and with a ring of Zry-4 holding the fast IPs.

7. Neutron fluxes

Knowledge of spatial distribution and spectrum of neutron flux is important for all applications. Neutron flux distribution is calculated at the BOC for the critical configuration (cylindrical shell-shaped control rod fully inserted) of the standard design. Three different z-planes are selected to visualize the asymmetry in neutron fluxes due to the asymmetry of the core. Fig. 7a–c, respectively shows the thermal neutron flux distribution as a color map over $z = 0$ plane (fluxes calculated in cubes of 1 cm^3), $z = 16$ cm plane

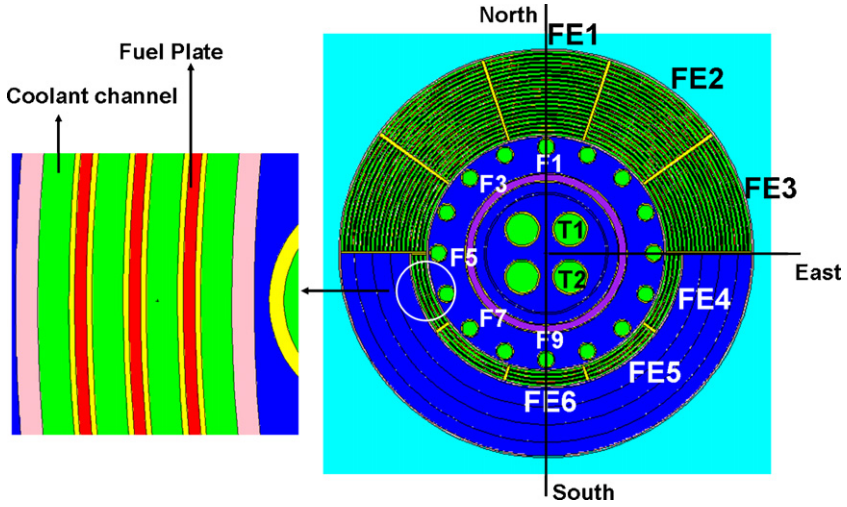

Fig. 6. Detailed heterogeneous asymmetric model. An enlarged view of a segment of the thin FE is shown on the left. FE, F and T initials refer to fuel element, fast irradiation position and thermal irradiation position, respectively.

Table 6
Dimensions and materials of the standard design and inner region (all dimensions are in cm).

Core	Inner radius	Outer radius	# FE
Thick section	10.0	17.164	5
Thin section	10.0	11.308 (padded with Be up to 17.164)	5
Structural Material (Zry-4)	9.85/10	17.164/17.314	-

FE	# Fuel plate	# Cooling channels per FE		Thickness	Material
			Meat	0.08 (radial direction)	U_3Si_2-Al
			Clad	0.038 (radial direction)	Al-6061
Thick	19	20	Cooling channel	0.21 (radial direction)	H_2O
Thin	3	4	Structural Material	0.15 (angular direction)	Al-6061

Inner region: Be + Control rod (cylindrical shell)					
	# of IP	Radius	Radial distance to core center	Clad thickness	Clad Material
Fast IP	16 (every 22.5)	0.65	9	0.15	Al-6061
Thermal IP	4 (every 45)	1.5	3	0.15	Al-6061
Control Rod (hafnium)	-	6.1/6.7	-	0.1	Al-6061

Table 7
Reactivity effects due to changes in the configuration of the inner-irradiation zone (changes involve entire active core height, 70 cm).

Case	k_{eff} at BOC (±0.04)
I – Base case (selected configuration)	1.168
II – Critical with Hafnium CR (6.1–6.7 cm)	1.000
III – Base case with heavy water filling the IPs	1.180
IV – Base case with air filling the IPs	1.165
V – Base case with Zry-4 ring (8–10 cm)	1.137

(fluxes calculated in parallelepipeds of $1 \times 1 \times 2\,cm^3$, x–y–z coordinates) and $z = 33$ cm plane (fluxes calculated in parallelepipeds of $1 \times 1 \times 4\,cm^3$). In Fig. 7, the center of the core is located at (x, y) = (0, 0), and the thick segment is located in the region of positive y-coordinate (top half of each cartoon). Note that the inner and outer radii of the core are shown in Fig. 7. A region of high thermal fluxes, appropriate for beam applications, exists outside the thicker fuel segment, in the heavy water reflector. Specifically, there is a volume of around 20 l with thermal neutron fluxes higher than $3.5 \times 10^{14}\,n\,cm^{-2}\,s^{-1}$ between the planes $z = \pm 16$ cm. The region outside the thin section of the core shows moderate fluxes that may be appropriate for industrial applications and/or irradiation devices that may get damaged under high neutron/photon fluxes. The region along the $y = 0$ line shows intermediate neutron flux levels ($2.5/3.0 \times 10^{14}\,n\,cm^{-2}\,s^{-1}$). The fast neutron flux is shown in Fig. 7d, only for the $z = 0$ plane (fluxes calculated in cubes of $1\,cm^3$). Fast neutron flux levels suggest that the fast irradiation positions should be located near the inner face of the thick segment of the core.

For a more quantitative feel, thermal neutron fluxes per MW along three different lines (north, east and south lines shown in Fig. 7) in the $z = 0$ and $z = 16$ planes are shown in Fig. 8. Also shown is the thermal neutron flux for the simplified model of the azimuthally symmetric FRM-II core. For the north-line in the cen-

Table 8
Characterization of fast and thermal irradiation positions (see Fig. 7).

Irradiation positions		Standard design						Zry-4 ring		
		Fast	Group 2	Epi.	Thermal	Fast/Th.	Epi/Th.	Tot/Tot	Fast/Th.	Epi/Th.
F1	C	2.43	1.79	0.92	0.87	2.80	1.06	1.01	4.88	1.32
	T	2.09	1.49	0.76	0.78	2.68	0.97	1.00	4.51	1.21
F3	C	2.19	1.64	0.83	0.92	2.38	0.91	0.98	4.59	1.37
	T	1.87	1.34	0.71	0.74	2.52	0.95	0.97	4.53	1.27
F5	C	1.66	1.32	0.68	0.79	2.11	0.87	0.96	3.75	1.17
	T	1.37	1.05	0.53	0.68	2.00	0.78	0.93	3.49	1.18
F7	C	0.97	0.82	0.46	0.72	1.35	0.64	0.88	2.23	0.86
	T	0.89	0.71	0.36	0.58	1.53	0.61	0.91	2.34	0.82
F9	C	0.85	0.75	0.37	0.58	1.47	0.65	0.84	2.04	0.80
	T	0.69	0.59	0.32	0.48	1.44	0.67	0.83	1.96	0.68
T1	C	0.81	0.83	0.46	0.93	0.87	0.50	0.82	0.74	0.48
	T	0.69	0.71	0.40	0.75	0.92	0.53	0.85	0.75	0.48
T2	C	0.57	0.64	0.40	0.79	0.72	0.51	0.78	0.58	0.44
	T	0.47	0.52	0.32	0.72	0.65	0.44	0.80	0.61	0.45

Fluxes are in $10^{14}\,n\,cm^{-2}\,s^{-1}$ units. Note that C indicates central plane ($z = \pm 2.5$ cm) and T indicates the location at $z = 17.5$ cm ($15 < z < 20$ cm).

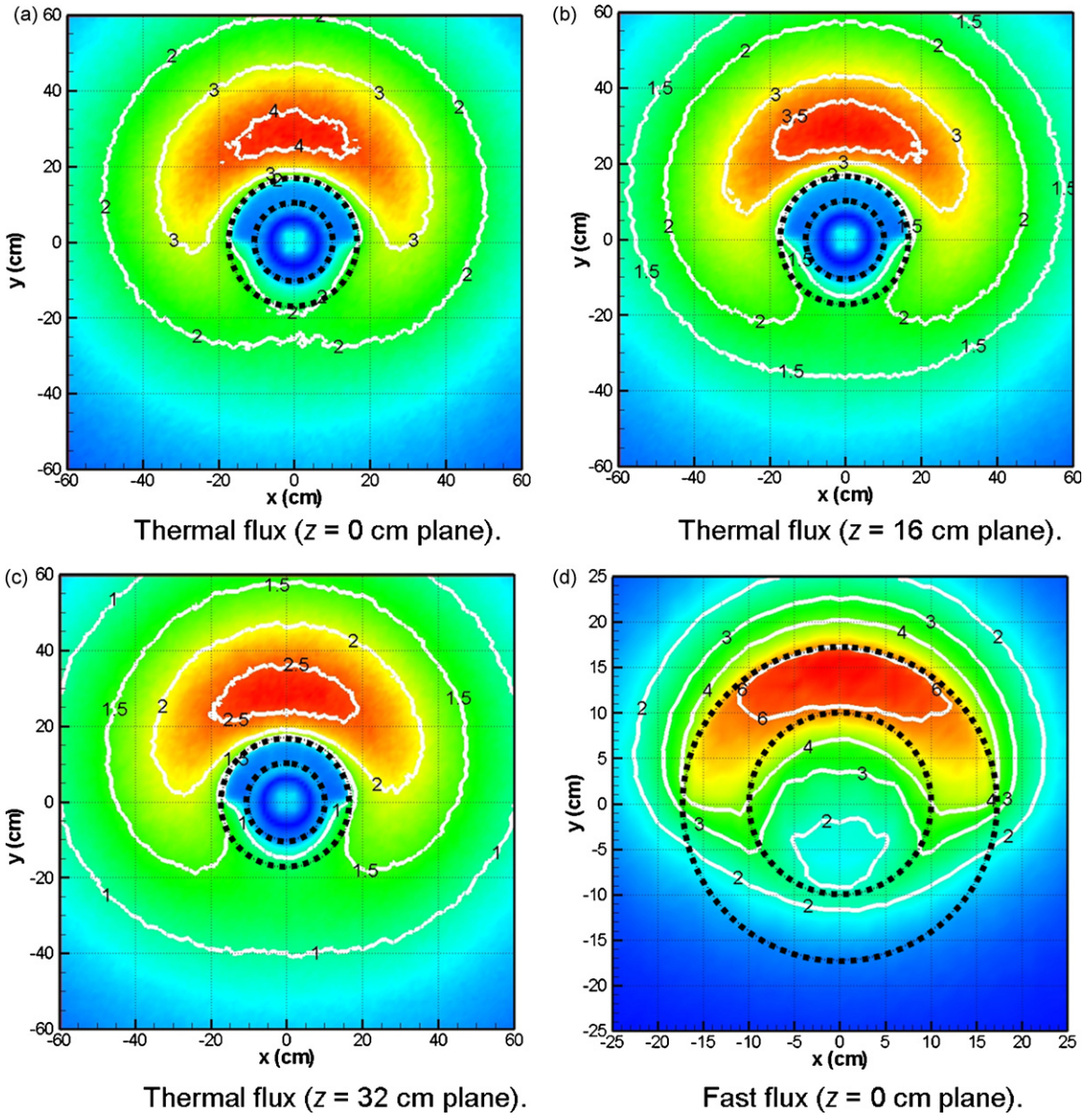

Fig. 7. Neutron flux distribution for the standard design (fluxes are in 10^{14} n cm^{-2} s^{-1} units). Note that the inner and outer radii of the core are shown in each picture. [Note also that the *x*–*y* range plotted in panel d is smaller than that in other figures.]

tral plane, results show a flux peak of 4.2×10^{14} n cm^{-2} s^{-1}, that is 5% higher than that calculated for the FRM-II case, located at 30 cm from the core center. Flux peaks of 3.0×10^{14} n cm^{-2} s^{-1} and 2.0×10^{14} n cm^{-2} s^{-1} occur along the east and south-lines, respectively. In the $z = 16$ plane, the MTF is reduced by about 10 and 15% with respect to the MTF on the central plane.

The inner region or inner reflector is included in the design to locate fast/thermal irradiation positions without affecting the thermal neutron flux in the heavy water reflector. The quality of these IPs is determined by the neutron spectrum as well as the neutron flux level. Following Ryskamp et al. (1991), neutron fluxes in four different energy groups are calculated for each IP at $z = 0$ (denoted by C in Table 8; cells between $z = \pm 2.5$ cm) and at another location 17.5 cm above the central plane (denoted by T; cells from $z = 15$ to 20 cm). Lower bounds for the four energy groups (fast, group 2, epithermal and thermal) are, respectively: 0.1 MeV, 100 eV, 0.625 eV and 0 eV. Fluxes are calculated not only for the standard design but also for Case V in Table 7, where the fast IPs are located in a Zry-4 ring and filled with air instead of light water. These two cases represent a broad range of flux levels in the IPs depending on the configuration. Table 8 shows neutron fluxes in each energy group and the ratios fast/thermal and epithermal/thermal for the standard design. The last three columns of Table 8 correspond to the standard design with a Zry-4 ring and air in the fast IPs. They show the total neutron flux relative to the standard design (total/total ratio) and the fast/thermal and epithermal/thermal ratios calculated for the standard design. Maximum fast fluxes are near the inner face of the central thick FE (FE1 in Fig. 6 and fast IP F1). Flux values start around 2.4×10^{14} n cm^{-2} s^{-1} (note that the neutron flux above the epithermal range is approximately 4.2×10^{14} n cm^{-2} s^{-1}) and decrease to about 8.5×10^{13} n cm^{-2} s^{-1} (F9).

A high value of fast/thermal flux is desirable. Ryskamp et al. (1991) assume as design criteria a value for this ratio not less than 0.5. The fast/thermal ratio for the base case, varies between 2.8 and 1.5 in different fast IPs, and between 4.8 and 1.9 in the Zry-4 ring case. Flux values are also shown for the thermal IPs (T1 and T2).

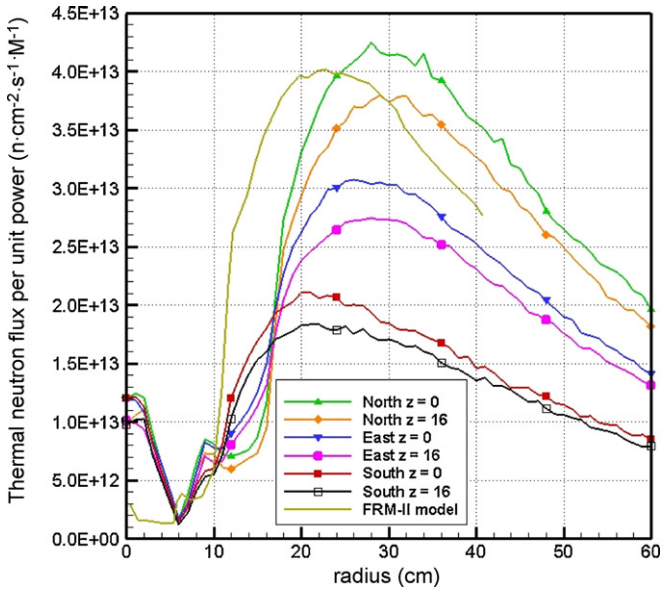

Fig. 8. Thermal neutron fluxes for the standard design (z = 0 and 16 cm) and for the simplified model of the FRM-II.

These locations may be considered as irradiation positions with an epithermal spectrum. It is important to mention that the central zone of the inner region, where T1 and T2 are located, is expected to be strongly affected by the final design of the inner region and by the positions of the control rods during the life cycle of the reactor.

8. Coolant outlet temperature and maximum fuel temperature

To further assess the viability of the design proposed here, it is important to compare thermal hydraulics and safety related parameters with those for the FRM-II reactor. The design under study is loaded with 4.65 kgU5 or 0.465 kgU5 MW^{-1}, whereas the FRM-II is loaded approximately with 0.375 kgU5 MW^{-1}. The core volume of the standard design is 24,400 cm^3 producing a power density of 409 W cm^{-3}. Corresponding value for the FRM-II core is 806 W cm^{-3}. Therefore, the proposed design produces half the power with approximately the same volume as the FRM-II core. Hence, in principle, this model is not expected to present any serious challenges from the core cooling point of view. From the safety point of view, the standard design has three different regions that may be suitable for control rod insertion: inner reflector, outer reflector (heavy water) and outer reflector surrounding the thin core segment (Be). These, together with the well-known shut down methods used in research reactors (poison, reflector drain, etc.), may allow several independent shut down systems.

The asymmetry of the core suggests that different FE may require different coolant conditions. To determine suitable coolant conditions for this design it is necessary to calculate the energy deposited in the core material when the reactor is at full power. This can be readily done with MCNP using a particular tally to account for the energy deposited by particles and fission products in the reactor material. For this purpose, a KCODE neutron–photon calculation of the standard design was carried out (1000 active cycles of 1000 histories per cycle). Results show that around 87% of the recoverable energy (~200 MeV $fission^{-1}$) is deposited in the core material, 0.2% is deposited in the inner region and the remaining energy is transferred to the heavy water reflector and surrounding materials. That is, for the 10 MW core design, 8.7 MW have to be removed by the coolant that flows through the core. The power density calculated

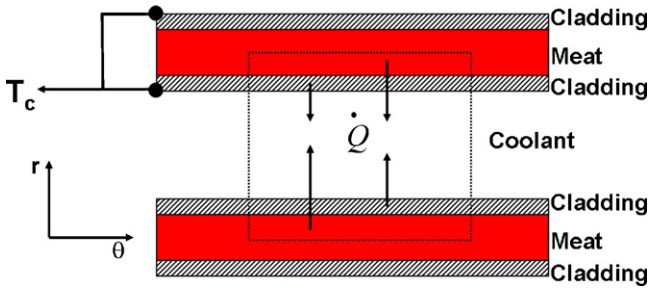

Fig. 9. Energy removed for each coolant channel (coolant flowing perpendicular to the page).

with the energy deposited in the core gives a total of 365 W cm^{-3} and 291 W cm^{-3} for the thick and thin segments, respectively.

With the help of a simple energy balance and assuming steady-state conditions, it is possible to calculate for each coolant channel the temperature rise of the coolant across the core. For each channel of each FE, a simple energy balance is carried out

$$\dot{Q} = \dot{m} C_p \Delta T \quad (1)$$

where $\dot{m}$ is the coolant mass flow rate, C_p is the specific heat of the coolant, ΔT is the coolant temperature rise across the core, and $\dot{Q}$ is the heat deposited in the core material per unit time. It is assumed that half of the energy deposited in the meat material of each fuel plate is transferred to each of the two coolant channels that sandwich the fuel plate (Fig. 9, horizontal cross section). All the energy deposited in the cladding material is assumed to be transferred to the coolant.

Assuming a coolant velocity of 8 m/s and an inlet temperature of 40 °C, Fig. 10 shows the outlet temperatures of the coolant channels for each FE. Note that channel 1 is the innermost channel. The FE of the thin segment of the core has only four coolant channels. The thicker part on the other hand consists of 20 coolant channels. Results show that channel #19 in FE1 is the hottest one, experiencing a temperature rise of 26 °C (see Fig. 6 for the FE number). Remaining FEs are not shown because of symmetry. The temperature rise of the coolant through the core is approximately 12 °C, and 14 °C for the hottest fuel element, FE1.

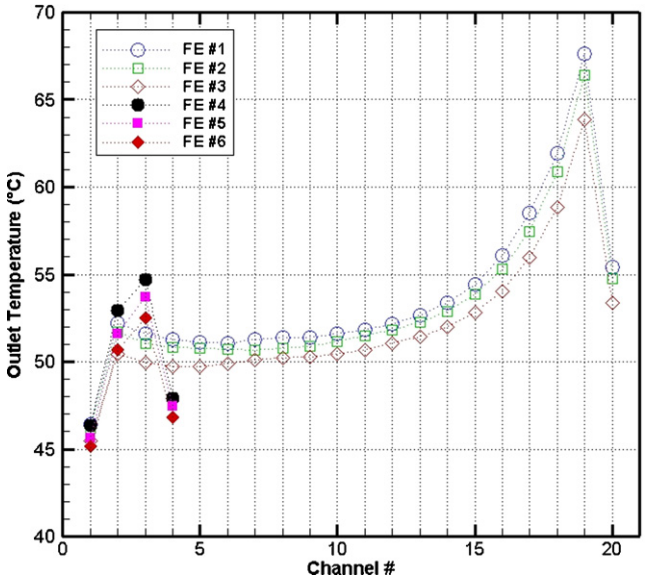

Fig. 10. Outlet temperature for each coolant channel in six fuel elements.

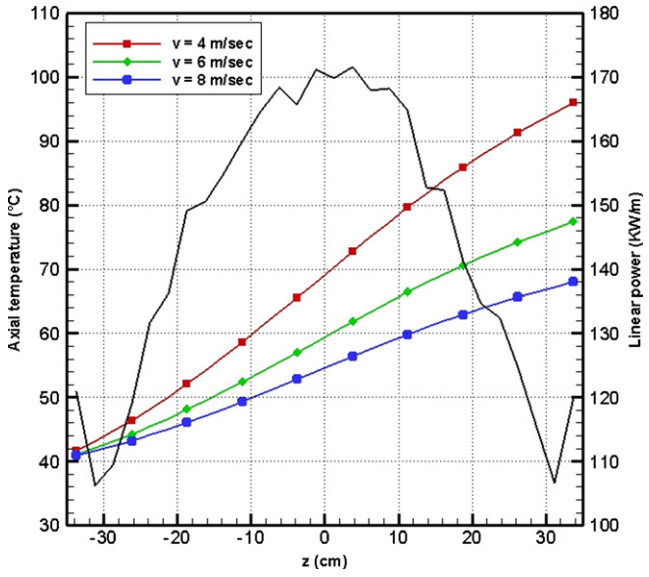

Fig. 11. Axial temperature profile and linear power for channel #19 in FE1.

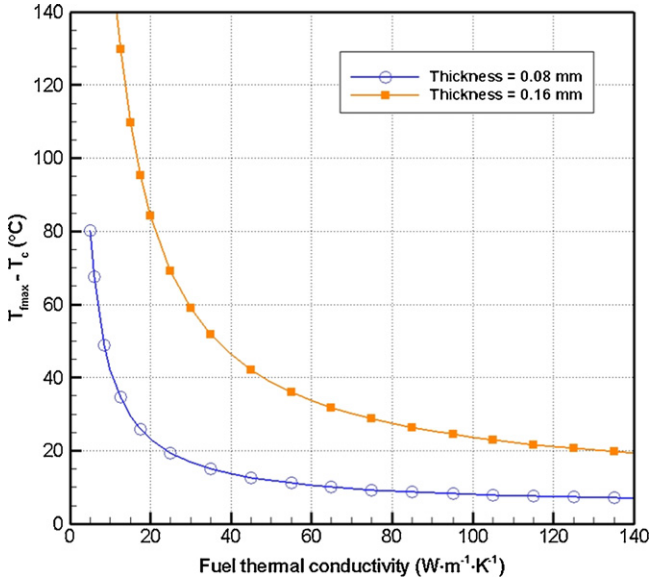

Fig. 12. Maximum fuel temperature as a function of the fuel thermal conductivity ($T_{fmax} - T_c$).

The coolant flow velocity is an important parameter that directly influences the coolant outlet temperature. The coolant velocity in FRM-II is about 16 m/s (Glaser, 2002). That means that the value used in the previous calculation (8 m/s) can be increased to values that have been tested in actual facilities for the same cooling channel area (0.21 cm per channel in the proposed design and 0.22 cm in FRM-II). The axial variation of the coolant temperature was calculated, with the coolant velocity as a parameter, for the hottest channel in our model (channel #19 in FE1, Fig. 10). The height of the channel was divided into 28 elements (2.5 cm each) and the energy deposited in each of these elements was calculated with MCNP. Axial and azimuthal heat conduction in the fuel plate is neglected. Fig. 11 shows the axial temperate profile for three different coolant velocities. The axial linear power distribution for this channel is also shown in Fig. 11. Clearly, for coolant velocities typical of research reactors, the temperature rise in the core and in the hottest channel remains safe. The CHF safety ratio can be conservatively calculated assuming a saturation temperature equal to 100 °C. With this assumption, the CHF ratio for the coolant velocities of 8, 6 and 4 m/s is: 1.07, 1.16 and 2.14, respectively. Compared to the FRM-II core, half of the power is being removed with approximately the same flow area and therefore, the thermo hydraulic design is less demanding than for instance in FRM-II. Although these are preliminary calculations, a flow velocity of around 8 m/s seems to be an acceptable value that results in safe coolant conditions and reduces pumping power.

Maximum fuel temperature is evaluated next. The thickness of the meat in the standard design (0.8 mm) is larger than that in the FRM-II facility (0.6 mm). To evaluate the maximum fuel temperature, the radial conduction equation in 1D cylindrical geometry is solved over the horizontal section of one fuel plate (Fig. 9). Axial and azimuthal heat conduction is neglected. The heat source is conservatively assumed to be uniform and equal to the maximum volumetric heat source calculated for the axial heat distribution of the hottest fuel plate (Fig. 11, center of the channel). Temperature distribution in the clad-meat-clad sandwich is calculated assuming the clad surfaces to be at the coolant temperature, T_c.

One of the key parameters in the calculation of the fuel temperature is its thermal conductivity. This parameter depends on the fuel fabrication process as well as on the burnup of the FE. An experimental correlation for the thermal conductivity of U_3Si_2–Al matrix as a function of the void space or porosity in the fuel is given by IAEA (1992). Although the thermal conductivity for standard fresh fuel can be assumed to be 180 W m^{-1} K^{-1}, for other porosities this can drop to values as low as 15 W m^{-1} K^{-1}. Therefore, as the porosity of the FE is not known *a priori*, the maximum fuel temperature is calculated as a function of the fuel thermal conductivity over the range of interest during the burnup cycle. Fig. 12 shows the maximum fuel temperature ($T_{fmax} - T_c$) as a function of the fuel thermal conductivity for two different meat thicknesses. Even with very low values of the fuel thermal conductivity (~10 W m^{-1} K^{-1}), the maximum fuel temperature is only 30–40 °C above the cladding surface temperature. As shown in Fig. 12, even if the meat thickness is doubled, maximum temperature values remain very low. Power density used in these calculations are 4800 W cm^{-3} and 10 W cm^{-3} for the meat and cladding, respectively.

9. A more compact core model

The standard design achieved the targets established at the outset: maximum thermal flux per unit power equal to the FRM-II core; capability to irradiate material with a hard spectrum; and a core life longer than 40 days. However, some of these requirements can be relaxed if even higher neutron flux is desired. A more compact model is developed to demonstrate that even higher neutron flux levels can be achieved with an asymmetric core. The general features and most dimensions of this compact design are the same as those identified earlier for the design analyzed in Sections 6–8. The main differences are in the inner region and in the dimensions of the core. There are no IPs in the inner region of the compact model, which is filled with Be. The core is made more compact compared to the design analyzed earlier. Inner reflector of this compact core is only 6 cm in radius compared to 10 cm for the core designed earlier. The thick half of the compact core extends from 6 cm to 13.5 cm of radius, while the thinner segment extends from 6 cm to 7.3 cm. The FEs have the same dimensions and number of channels as described in Table 5 except that the meat thickness is increased to 0.11 cm to increase the excess reactivity at BOC. Note that the two 180° segments of the core are also slightly thicker than in the earlier design. The core volume is approximately 18,800 cm^3, loaded with 4.5 kg of U5 and with a nominal power density of 530 W cm^{-3}.

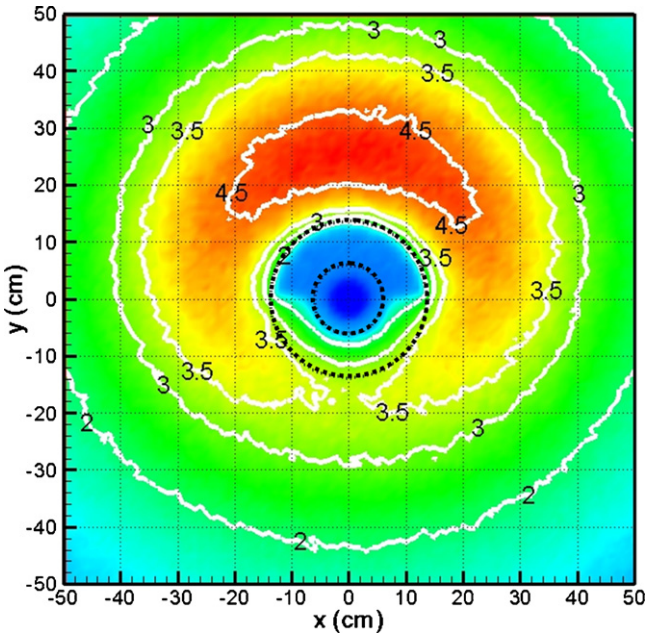

Fig. 13. Neutron flux distribution for the heterogeneous compact model (fluxes are in 10^{14} n cm^{-2} s^{-1} units) in the central horizontal plane. Note that the inner and outer radii of the core are shown in the picture.

Thermal neutron fluxes for the compact core are shown in Fig. 13. A maximum flux of 5.0×10^{14} n cm^{-2} s^{-1} is achieved along the north line in the central plane together with maximum fluxes of 4.0×10^{14} n cm^{-2} s^{-1} and 3.0×10^{14} n cm^{-2} s^{-1} along the east and south lines, respectively. This model shows a MTF per unit power which is 25% higher than that in the FRM-II design. Fluxes are calculated for the critical configuration at the BOC.

The heterogeneous model shows an excess reactivity at BOC equal to $\Delta k = 12.5\%$. The model is made critical at BOC with a cylindrical shell made of hafnium that extends from 2 cm to 3.25 cm in the radial direction. A homogeneous model is simulated using the MONTEBURNS package to evaluate the core life. Assuming the same reactivity variation with burnup in the heterogeneous case as in the homogenous one, the marginal reactivity after 23 days of operation results in $\Delta k = 6.3 \pm 0.5\%$.

Another design feature of interest in the compact core is the area in the reflector available to locate facilities that require a specified neutron flux level. Table 9 shows the comparison of areas in the reflector with thermal fluxes greater than 2.0, 3.0, 3.5 and 4.5×10^{13} n cm^{-2} s^{-1} MW^{-1} for the simplified model of FRM-II, the standard design, and the compact design described in this section. The compact core, at the expense of a shorter core life, yields larger MTF as well as larger areas where this level of flux is available than the FRM-II design.

Table 9
Areas (cm^2) in the central plane ($z = 0$) satisfying thermal flux level requirements.

Thermal flux	FRM-II simplified model	Standard design	Compact core
>2.0×10^{14} n cm^{-2} s^{-1} MW^{-1}	7440	6200	7830
>3.0×10^{14} n cm^{-2} s^{-1} MW^{-1}	3920	2180	4420
>3.5×10^{14} n cm^{-2} s^{-1} MW^{-1}	2410	1070	2780
>4.5×10^{14} n cm^{-2} s^{-1} MW^{-1}	–	–	490

10. Comments and concluding remarks

To increase the intensity of the neutron source new research reactor designs generally rely on increasing power. However, high power levels imply large-scale projects that may not be economically feasible or may not be suitable if the research reactor is intended to be built at an educational institution. The design effort reported here was motivated by the desire to achieve high flux levels per MW with LEU fuel in a medium sized research reactor. A novel, asymmetric design of a reactor core has been proposed. The azimuthal asymmetry, not found in existing facilities, leads to a region in the reactor that may have higher flux levels than maximum flux level in an azimuthally symmetric design. This region in a RR of moderate power level is suitable to locate experimental devices that require high neutron fluxes (note also that though the design power level is selected as 10 MW, the concept of the asymmetric core is independent of the power level). Two asymmetric designs have been analyzed. First design, called the "standard design," has been analyzed in much more detail than the second one called the "compact design."

The standard design is a 10 MW annular asymmetric cylindrical core. The core is loaded with standard 20% enriched fuel. The maximum thermal flux levels are comparable to levels existing in state of the art facilities. The unperturbed thermal peak per unit power is comparable to that in the FRM-II and the core life is estimated to be around 41 days (depending on the facilities located in the heavy water reflector). The asymmetric design leads to a high thermal neutron flux zone (4.2×10^{14} n cm^{-2} s^{-1}), a moderate thermal neutron flux zone (3.0×10^{14} n cm^{-2} s^{-1}), and a low thermal neutron flux zone (2.0×10^{14} n cm^{-2} s^{-1}) in the outer reflector. Each region may be suitable for facilities and devices with different flux requirements. Moreover, there is also an inner-irradiation area suitable for fast irradiation positions. This region consists of 16 IPs where the maximum fast neutron flux is 2.4×10^{14} n cm^{-2} s^{-1}. Fast/thermal ratio ranges from 1 to 3 in different irradiation locations. The asymmetry of the core is not expected to lead to any major operational or safety concerns. Moreover, reactivity control mechanism can be relatively effectively instituted in the rather large space around the core.

Steady-state thermo hydraulic analysis shows that the proposed design generates half the power of the FRM-II reactor in the same volume and with similar geometric parameters. Therefore, safety related systems developed for the FRM-II core are expected to be suitable for the design proposed here. Although further studies are required, preliminary thermal hydraulic analyses were carried out in this work. With a coolant velocity of 8 m/s, the temperature rise of the coolant through the core was found to be 12 °C. The same quantity calculated in the hottest channel is 26 °C. Although coolant velocity of 8 m/s, or even 6 m/s, may be sufficient for reactor safety, this quantity can be increased substantially, as for instance in the FRM-II reactor (16 m/s), without expecting any adverse mechanical or material impact on the core. A simplified model was developed to obtain an estimate of the maximum temperature inside the fuel material under full power operation. Given the design and material of fuel plates commonly used in research reactors, maximum temperatures exceed the coolant temperature by no more than 40 °C, even when considering the worst case for the fuel thermal conductivity. Although models employed to calculate steady-state thermal hydraulic parameters are simple, maximum temperatures calculated are sufficiently low to assure that steady-state thermo hydraulic analysis is unlikely to be the limiting factor for this design.

To further explore the potential of the asymmetric model, a more compact core was also analyzed. This compact core does not have an inner region for fast irradiation positions. Maximum thermal flux per unit power in the compact core (5.0×10^{13} n cm^{-2} s^{-1} MW^{-1})

is 25% higher than that obtained in the FRM-II together with an estimated core life of about 23 days. A shorter core life is a limiting factor for the compact core which is expected to be addressed with the development of new fuel materials with higher uranium densities.

Acknowledgement

This research was supported by an INIE grant from the Department of Energy.

References

Bonning, K., Petry, W., Rohrmoser, A., Morkel, Chr., Wieschalla, N., 2004. Conversion of the FRM-II. Research Reactor fuel Management, Munich, Germany.
Croff, A.G., 1980. User's Manual for the ORIGEN2 Computer Code. Oak Ridge National Laboratory.
FRM-II, 2008. Available via web at http://www.frm2.tum.de/en/technik/index.html/.
Glaser, A., 2002. The conversion of research reactors to low-enriched fuel and the case of the FRM-II. Science and Global Security 9, 61–79.
Hanan, N.A., Mo, S.C., Smith, R.S., Matos, J.E., 1996. An Alternative LEU Design for the FRM-II. ANL/RERTR/TM-27.
IAEA, 1999. Available via web at http://www.iaea.org/worldatom/rrdb/.
IAEA, 1992. Research Reactor core conversion guidebook. Volume 4: fuels (appendices I–K). IAEA-TECDOC-643.
MCNP5, 2003. MCNP-A General Monte Carlo N-Particle Transport Code, Version 5. LA-CP-03-0245, Los Alamos National Laboratory.
OPAL, 2008. Available via web at http://www.ansto.gov.au/discover/opal_reactor.html/.
Poston, D.I., Trellue, H.R., 1999. User's Manual, Versión 2.0 for Monteburns, version 1.0. Los Alamos National Laboratory.
RERTR, 2008. Available via web at http://www.rertr.anl.gov/.
Ryskamp, J.M., Selby, D.L., Primm III, R.T., 1991. Reactor design of the advance neutron source. Nuclear technology 93, 330–349.
Teruel, F., Rizwan-uddin, 2005. An alternative model for neutron flux maximization in research reactors. In: Proceeding of the International Topical Meeting of Mathematics and Computation, Supercomputing, Reactor Physics and Nuclear and Biological Applications, Avignon, France, September 12–15.
Teruel, F., Rizwan-uddin, 2006. Detailed core design and flow coolant conditions for neutron flux maximization in research reactors. In: Proceeding of International Conference on Nuclear Engineering, Miami, USA, July 17–20.